

Figure S1. Chemicals and conditions used to obtain worm populations developing continuously through L2d trajectory. Related to Figure 2.

(A-B) Molecular structures (using www.molview.org), names, and CAS numbers of the chemicals used in the ascaroside (dauer-inducing), and ascaroside plus dafachronic acid (both dauer-inducing and dauer commitment inhibiting) plates.

(C) Two different concentrations of Ascrs assayed in combination with four different concentrations of dafachronic acid (DA) to determine conditions that prevent dauer formation in the presence of ascarosides. Percent dauer formation in the presence of different combinations of ascarosides (Ascrs: equimolar mixture of ascr#2, ascr#3, and ascr#5) and DA are plotted. DA inhibits dauer commitment but not L2d, which is evident by slowing of larval development. The combination of 3 μM of Ascrs and 0.03 μM DA was used as the L2d-inducing (Ascrs+DA) condition to test the effect of the L2d trajectory on the number of seam cells in wild-type and *mir-48/84/241* animals (Figure 2).

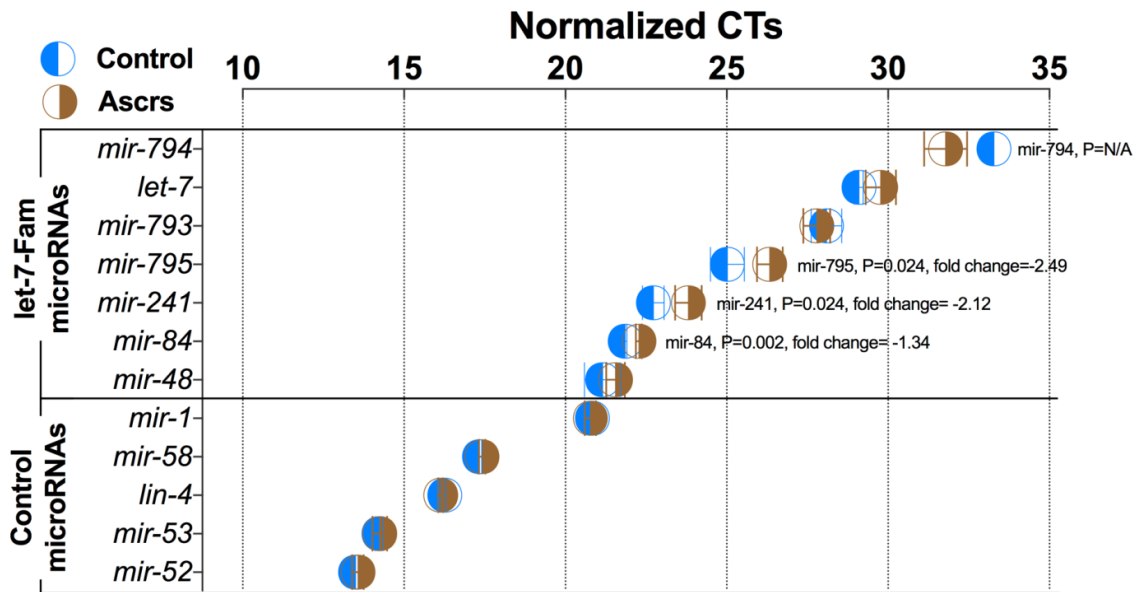


Figure S2. Ascarosides do not result in an increase in *let-7* family levels in *daf-12(rh61)* background. Related to Figure 2.

let-7 family microRNAs in L2-to-L3 (control) vs. L2d-to-L3 (Ascros) molting larvae of the *daf-12(rh61)* mutant were quantified using Taqman assays as described in the STAR methods. MicroRNAs that are highly expressed and not environmentally regulated were used as the normalization set (Control MicroRNAs). The expression levels of three *let-7* family microRNAs (*mir-84*, *mir-241*, *mir-795*) were slightly but statistically significantly reduced in the presence of ascarosides (L2d-to-L3 molt). This reduction of *let-7* family levels is in contrast with the observed suppression of retarded heterochronic phenotypes of *daf-12(rh61)* in the presence of ascarosides. The lack of an upregulation of *let-7* family microRNAs in the presence of ascarosides is in line with the idea that an alternative, *let-7*-independent, mechanism is responsible for the ascaroside-mediated suppression of the heterochronic phenotypes. *mir-794* was not detected in two biological control samples (presumably due to low expression level); therefore, we do not know if there is a statistically significant up-regulation of *mir-794* in the presence of ascarosides.

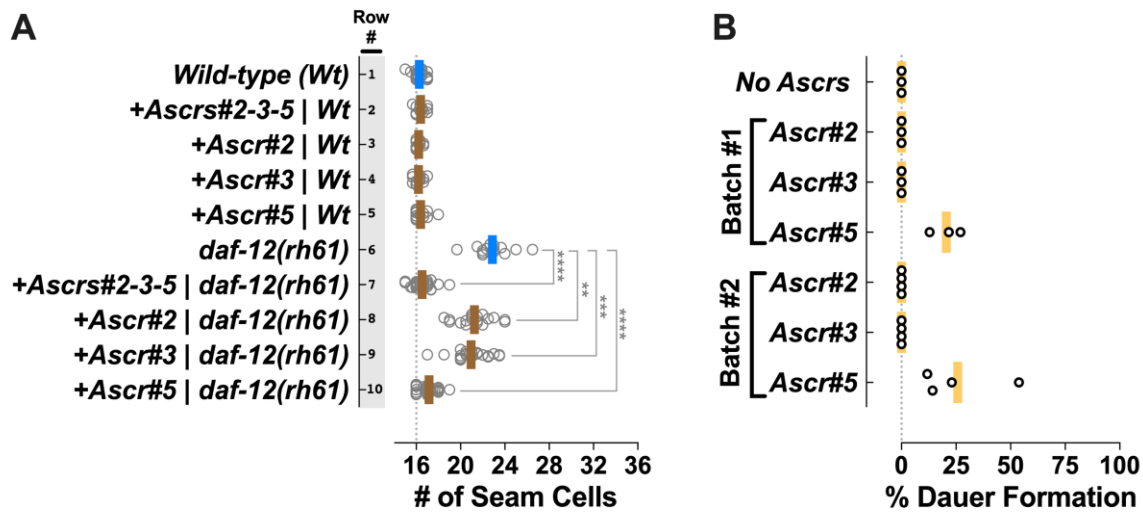


Figure S3. Testing of individual components of the pheromone cocktail for their potencies to suppress the extra seam cell phenotypes of *daf-12(rh61)* and to induce dauer formation. Related to Figure 3.

(A) Individual components of the pheromone cocktail can suppress the extra seam cell phenotypes of *daf-12(rh61)* and *ascr#5* is the most potent suppressor. Number of seam cells in young adult animals cultured under different ascaroside conditions are plotted. Each dot in the plot shows the number of seam cells of a single young adult animal, and solid lines (blue: rapid trajectory; brown: delayed [12d] trajectory) indicate the average seam cell number of the animals scored for each condition. Ascrs#2-3-5 plates contained all three ascarosides at 3 μ M final concentration of each ascaroside mixed in NGM-agarose media. Ascrs#2, Ascr#3, and Ascr#5 plates contained 3 μ M final concentration of each ascaroside mixed in NGM-agarose media. The student's t-test is used to calculate statistical significance (p): n.s. (not significant) $p > 0.05$, * $p < 0.05$, ** $p < 0.01$, *** $p < 0.001$, **** $p < 0.0001$

(B) Ascr#5 alone can induce dauer formation. At 3.3 μ M concentration, using agarose NGM plates with no peptone, seeded with washed and concentrated *E. coli* OP50 culture as described in the STAR methods, Ascr#5 alone was sufficient to induce dauer formation but not Ascr#2 or Ascr#3. We tested single ascarosides in two different batches of plates and using three or four replicates. Both experiments were performed at 20°C. Each dot on the plots shows percent dauer formation on a single plate. We maintained population sizes small (<55 worms per plate) and comparable across different Ascr plates to minimize the potential effect of the accumulation of ascarosides secreted by the worms on the plates.

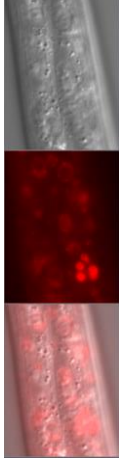

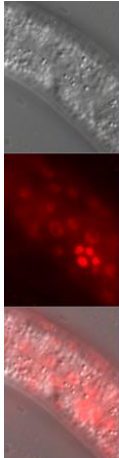
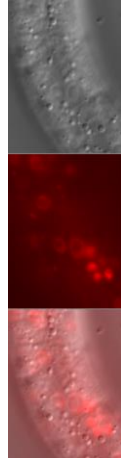

Time (Hours)	10	22	29	36	44
Genotype	<i>hbl-1(ma430[hbl-1::mScarlet-I])</i>				
Stage	L1	Late L2	L3	L4	Adult
HBL-1 Expression (# of animals scored)	Yes (10/10)	Yes (10/10)	No (0/10)	No (0/10)	No (0/10)
Example Pictures	n/a			n/a	n/a
Genotype	<i>daf-7(e1372); hbl-1(ma430[hbl-1::mScarlet-I])</i>				
Stage	L1	L2d	Late L2d	L3	L4
HBL-1 Expression (# of animals scored)	Yes (10/10)	Yes (10/10)	Yes (10/10)	No (0/10)	No (0/10)
Example Pictures	n/a				n/a

Figure S4. HBL-1 is present throughout the L2 or the lengthened L2d stage but it is absent at the post-L2 or post-L2d L3 stage. Related to Figure 5.

Endogenously tagged HBL-1 expression was examined in wild-type and *daf-7(e1372)* backgrounds at 20°C. *daf-7(e1372)* animals form dauer larvae at 25°C but they develop continuously going through L2d at 20°C. For each time point and genotype ten animals were examined. In all animals at 22 hours, also in *daf-7(e1372)* animals at 29 hours, L2 stage specific V5p cell divisions were observed to have occurred (a cluster of four small and bright nuclei in each picture), indicating that the animals were at a late phase of the L2 stage. In L2d animals the lengthening of the second larval stage appeared to occur after the execution of these L2 stage cell divisions. HBL-1 is detected in late L2 and L2d larvae but it was not detected in post-L2 and post-L2d L3 stage larvae, indicating that the duration of HBL-1 expression is lengthened as the L2 stage is lengthened during L2d, and in both post-L2 L3 and post-L2d L3 animals HBL-1 is downregulated.

Strain name	Genotype	Related figure(s)
VT1367	<i>mals105[pCol-19::gfp] V</i>	Figure 2, 3B, 3C, 3D, S1
VT1453	<i>mir-48 mir-241(nDf51) mals105 V; mir-84(n4037) X</i>	Figure 2
VT791	<i>mals105 V; daf-12(rh61) X</i>	Figure 2, 3, 4, S2, S3
VT2962	<i>daf-7(e1372) III; mals105 V; daf-12(rh61) X</i>	Figure 2, 3C, 3E
VT3568	<i>daf-2(e1370) III; mals105 V; daf-12(rh61) X</i>	Figure 2, 3D, 3E
VT3135	<i>mals105 V; srg-36srg-37(kyIR95) daf-12(rh61) X</i>	Figure 3A
VT2972	<i>mals105 V; daf-3(mgDf90) daf-12(rh61) X</i>	Figure 3B, 3C
VT1308	<i>daf-7(e1372) III; mals105 V</i>	Figure 3C
VT1755	<i>mals105 V; daf-3(mgDf90) X</i>	Figure 3C
VT1747	<i>daf-7(e1372) III; mals105 V; daf-3(mgDf90) X</i>	Figure 3C
VT2984	<i>daf-7(e1372) III; mals105 V; daf-3(mgDf90) daf-12(rh61) X</i>	Figure 3C
VT1776	<i>daf-2(e1370) III; mals105 V</i>	Figure 3D
VT3566	<i>daf-16(mgDf50) I; mals105 V</i>	Figure 3D
VT3567	<i>daf-16(mgDf50) I; daf-2(e1370) III; mals105 V</i>	Figure 3D
VT3569	<i>daf-16(mgDf50) I; mals105 V; daf-12(rh61) X</i>	Figure 3D
VT3570	<i>daf-16(mgDf50) I; daf-2(e1370) III; mals105 V; daf-12(rh61) X</i>	Figure 3D
VT3682	<i>daf-16(mgDf90) I; daf-7(e1372) III; mals105 V</i>	Figure 3E
VT3681	<i>daf-2(e1370) III; mals105 V; daf-3(mgDf90) X</i>	Figure 3E
VT3684	<i>daf-16(mgDf90) I; daf-7(e1372) III; mals105 V; daf-12(rh61) X</i>	Figure 3E
VT3683	<i>daf-2(e1370) III; mals105 V; daf-3(mgDf90) daf-12(rh61) X</i>	Figure 3E
VT2952	<i>mals105 V; daf-9(m540) daf-12(rh61) X</i>	Figure 3F
VT3061	<i>wIs51[pScm::gfp] V; daf-12(rh61rh411) X</i>	Figure 3G
VT3057	<i>din-1(dh127) II; mir-48 mir-241(nDf51) mals105 V</i>	Figure 3H
VT3894	<i>daf-12(rh61) hbl-1(ma430[hbl-1::mScarlet-I] X</i>	Figure 4A
VT3895	<i>daf-7(e1372) III; daf-12(rh61) hbl-1(ma430[hbl-1::mScarlet-I] X</i>	Figure 4A
VT2086	<i>lin-46(ma164) mals105 V; mir-84(n4037) X</i>	Figure 4B
VT1065	<i>lin-4(e912); lin-14(n179) mir-84(n4037) X</i>	Figure 4C
VT3030	<i>nhl-2(ok818) III; mals105 V; daf-12(rh61) X</i>	Figure 4D
VT3751	<i>mals105 V; hbl-1(ma430[hbl-1::mScarlet-I] X</i>	Figure S4
VT3893	<i>daf-7(e1372) III; hbl-1(ma430[hbl-1::mScarlet-I] X</i>	Figure S4

Table S1. *C. elegans* strains used in this study. Related to Figure 2, 3, 4 and 5.

All gene, allele, and transgene names, and chromosome numbers are italicized (Genotype column). *mals105* and *wIs51* are integrated extrachromosomal arrays expressing *pCol-19::gfp* and *pScm::gfp* to mark hypodermal cells of adult stage animals and hypodermal seam cells at all stages, respectively. All figures related to each strain are listed in the related figures column.

Primer #	Primer name	Primer Sequence (5' to 3')	Used for
1	Forward (pOI301)	gtttaagagctatgctggaacagcatagcaagttaaataaggctagtcgg	To generate pOI83 by modifying the tracr sequence of pRB1017
2	Reverse (pOI302)	agagaccgagtagcgggttctc	
3	Forward (priOI316)	tctgaagccagacaccaataatg	Cloning of pOI89 – <i>hbl-1</i> (<i>sgRNA</i>)
4	Reverse (priOI317)	aaaccattattggtgtctggcttc	
5	Forward (priOI323)	tcttgaaccggtgccgaatacac	Cloning of pOI91 – <i>unc-22</i> (<i>sgRNA</i>)
6	Reverse (priOI324)	aaacgtgtattcggcaacgggttc	
			Cloning of pOI191- HR template
7	Forward (priOI670)	gaaggtctcatctggagggtgatctggagggtgatctggagggtgatctgtcagcaagggagagggcagttatc	To amplify <i>mScarlet</i> from pSEM91 and to fuse with a linker
8	Reverse (priOI671)	gaaggtctcactttagagctcgtccattcc	
9	Forward (priOI672)	gaaggtctcacaagtaatgaggacgtcctcgttaagg	To amplify a fragment containing the HR arms+ plasmid backbone from pOI115
10	Reverse (priOI673)	gaaggtctcacagattggtgtctggcttggtacat	
11	Forward (priOI705)	cccacaattcatgtacggatcccgtgccttcatcaagcaccagccg	To convert <i>mScarlet</i> to <i>mScarlet-I</i> using SDM (T74I = acc>atc)
12	Reverse (priOI706)	gagaggatgtcccaggagaat	
13	Left Arm-Forward (priOI342)	cgggaattcaagatggcgagtaagcgt	To clone the HR arms for the assembly of pOI115 (these primers define the ends of the HR arms)
14	Right arm – Reverse (priOI343)	gccggatccaacaagtattctgggggaggt	
15	Forward (priOI262)	tcacccggagacgaggagac	Screening of F1 progeny of CRISPR mix injected P0 worms for HR (<i>hbl-1::mScarlet-I</i>) events
12	Reverse (priOI706)	gagaggatgtcccaggagaat	
15	Forward (priOI262)	tcacccggagacgaggagac	Screening of F2 progeny of F1 worms positive for HR events – these primers flank the HR arms
16	Reverse (priOI228)	aaaagagcagcagagttgg	

Table S2. Primers used in this study. Related to STAR Methods.